Elsevier Editorial System(tm) for Acta Biomaterialia

Manuscript Draft

Manuscript Number: AB-16-247R2

Title: Strontium (Sr) elicits odontogenic differentiation of human dental pulp stem cells (hDPSCs): a therapeutic role for Sr in dentine repair?

Article Type: Full length article

Keywords: Strontium (Sr), human dental pulp stem cells (hDPSCs), odontogenic differentiation, dentine sialophosphoprotein (DSPP), dentine matrix protein 1 (DMP-1), bioactive glass (BG), dentine, CaSR, MAPK/ERK.

Corresponding Author: Miss. Mei Huang,

Corresponding Author's Institution: Queen Mary University of London, Barts & The London School of Medicine and Dentistry, Blizard Building

First Author: Mei Huang

Order of Authors: Mei Huang; Robert Hill; Simon Rawlinson

Abstract: Strontium (Sr) forms a significant component of dental restorative materials and although it is widely used in toothpastes, the biological effects of Sr on the dentine-pulp complex have not been investigated. In this first study, we characterise the Sr elicited effects on human dental pulp stem cells (hDPSC) in vitro using exogenously Sr added to culture medium, and bioavailable Sr derived from a novel bioactive glass (BG). The related mechanisms were also investigated. Our results indicate that low dose Sr (between 0.1 and 2.5 mM) induces proliferation and alkaline phosphatase (ALP) activity of hDPSCs, but has no effect on colony formation or cell migration. Sr at specific concentrations (1 and 2.5 mM) stimulated collagen formation and mineralisation of the hDPSC generated matrix. In addition, qRT-PCR, Western blotting and immunocytochemistry revealed that Sr regulates gene expression and the protein secretion of the odontogenic markers: dentine sialophosphoprotein (DSPP) and dentine matrix protein 1 (DMP-1) and protein localisation (DSPP was localised to the Golgi, while no apparent changes occur in DMP-1 distribution which remains in both cytosol and the nucleus). Additionally, the calcium sensing receptor (CaSR) and downstream pathway MAPK/ERK signaling pathway in hDPSCs were activated by Sr. Bioavailable Sr from the BG revealed novel biological insights of regulating metabolic and ALP activities in hDPSCs. Taken together, these results suggest that Sr at specific doses significantly influences proliferation, odontogenic differentiation and mineralisation of hDPSCs in vitro via the CaSR using a pathway with similarities to osteoblast differentiation. These are the first such studies and indicate that Sr treatment of hDPSCs could be a promising therapeutic agent in dental applications. In conclusion, we propose that Sr from a substituted BG could be used more effectively in biomaterials designed for dental applications.

***Statement of Significance**

Despite the fact that strontium (Sr) is used widely in dental practice, its potential effects on odontoblasts have been ignored. Our study provides the first evidence that Sr (exogenous and that derived from a bioglass (BG)) can stimulate dentinogenesis in dental pulp stem cells (DPSCs) by promoting their proliferation, differentiation and mineralisation in vitro. Therefore, whilst previously unrecognised, Sr BG is likely to be beneficial in atraumatic dentistry practise and maintenance of a competent tooth in conditions such as caries. Repair of defected dentine is still one of the main challenges in dental research and annually untreated caries results in the loss of productivity equivalent to US$ 27 billion. Advances in tissue engineering technology, alongside the use of dental pulp stem cells provide an approach to achieve dentine regeneration. Understanding the actions of Sr will permit a more controlled application of Sr in the clinic. These data are thus likely to be of great interest to the material scientists, biological researchers, clinicians and manufacturers of dental products.

*Graphical Abstract

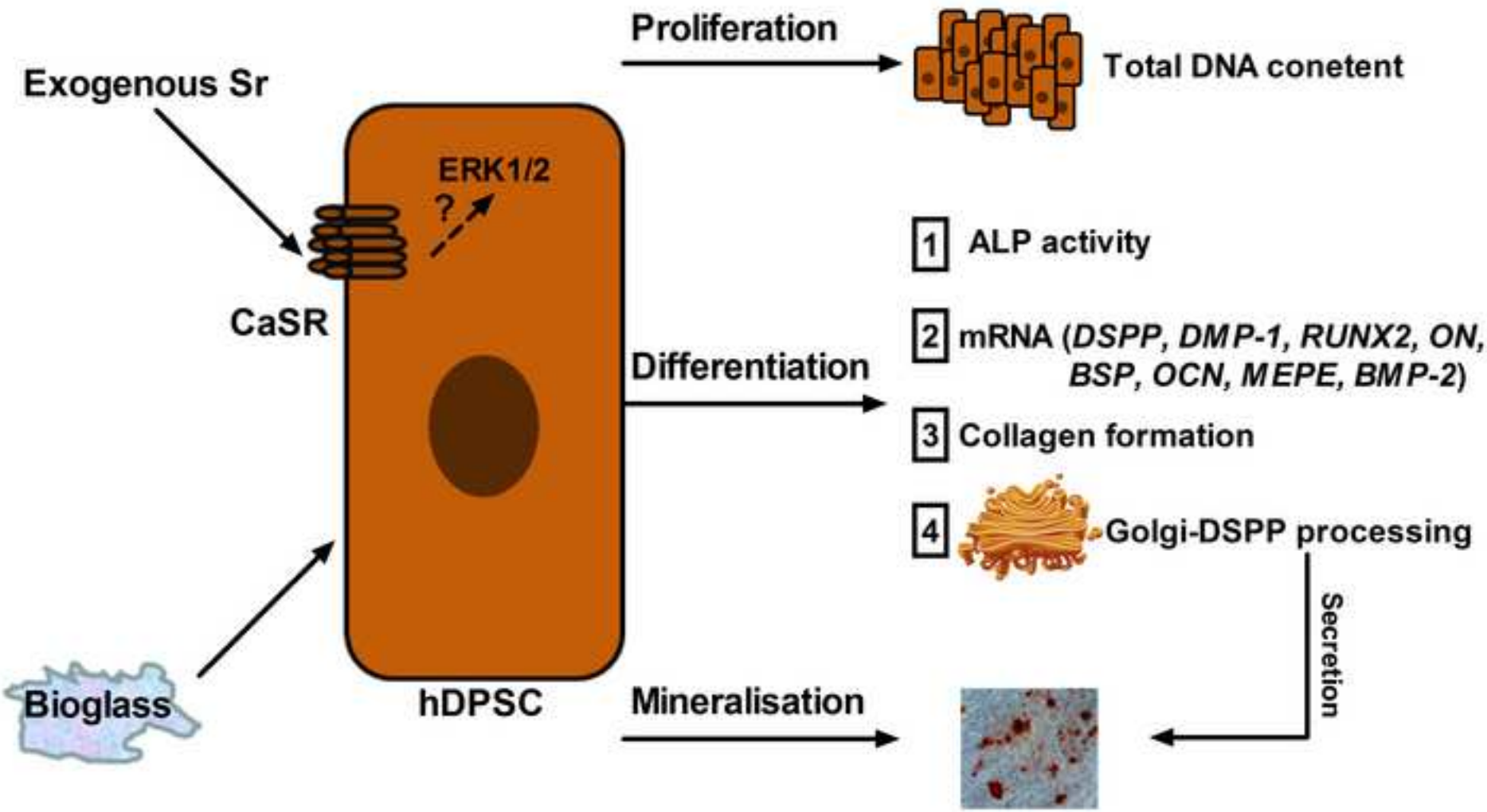

Strontium (Sr) elicits odontogenic differentiation of human dental pulp stem cells (hDPSCs): a therapeutic role for Sr in dentine repair?

1. Introduction:

Dentine is a major constituent of teeth and it protects the dental pulp – which, in turn, primarily provides nutrition and acts as a biosensor to detect potential pathogenic stimuli [1]. Carious defects in dentine and loss of enamel may affect the pulp viability with subsequent decreases in tooth strength and increased fragility. Preservation of the dentine mass is therefore crucial for maintaining the whole tooth.

Annually, untreated caries results in the loss of productivity equivalent to US$ 25.14 billion for permanent teeth, and US$2.09 billion for deciduous teeth [2]. Recent advancement in tissue engineering technology provides an approach to achieve dentine regeneration by replacement or repair of the impaired dentine-pulp tissues [3]. There are three key factors for optimal tooth tissue engineering: growth factors, suitable biomaterials and responsive stem/progenitor cells [4]. A unique population of postnatal human dental pulp stem cells (hDPSCs) from human adult dental pulp tissue have been characterised by Gronthos et al [5]. These cells demonstrate characteristic stem cell properties, and also show rapid proliferative rate, as well as the capacity to form mineralised dentine-like tissue both *in vivo* and *in vitro* [5, 6]. Due to their regenerative potential, the use of hDPSCs in dental regeneration is favoured [7-9]. A range of materials have been studied in the regeneration of hard dental tissues, including hydrogel scaffolds [10], degradable synthetic polymers [11], bioceramics [12], as well as mineral trioxide aggregate (MTA) [13]. However, whilst these materials have beneficial effects, none are perfect; therefore new biomaterials that possess more appropriate properties and bioactivity remain to be identified.

Strontium (Sr), in trace amounts, is a normal constituent of tooth structure. However, following capping of dental pulp in dogs using strontium hydroxide ($Sr(OH)_2$), Sr was identified in the dental pulp[14, 15]. As a result of its low systemic toxicity and high atomic number Sr-based materials are widely used in dental materials in the clinic to locate the restorations by X-ray. Additionally, Sr is added as an active agent of dentifrices for treating dentine hypersensitivity. Originally, strontium chloride ($SrCl_2$) was used in dentifrices but more recently strontium acetate ($Sr(C_2H_3O_2)_2$) at a loading of 8% w/w has been used. Sr is also used as a component of many dental restoratives to repair decayed teeth, particularly in glass ionomer cements, such as Fuji IX® (GC, Japan) which has the composition: 12.9%Al - 22.5% Si- 1.7%P - 0%Ca - 12.6%F - 5.6%Sr [16]. In these cases, Sr is in close association with exposed dentinal tubules. Occlusion of these tubules, and with high external Sr concentration, there is the potential for Sr to traverse internally and reach the pulp cavity. Given the widespread dental use of Sr, it is surprising that so little is known regarding its biological activity on odontoblasts.

It is well known that Sr can alter pre-osteoblast/osteoblast behaviour to induce mineralised bone-like nodules [17]. Recently, Strontium ranelate ($C_{12}H_6N_2O_8SSr_2$, at 1-2 g/day) has been approved for osteoporosis therapy. The related molecular mechanisms by which Sr regulates osteoblasts, include the calcium sensing receptor (CaSR) and CaSR-downstream pathway, such as mitogen-activated protein kinase (MAPK) signalling pathway [18] and Wnt/β-catenin signalling pathway [19]. Osteoblasts and odontoblasts both produce an extracellular matrix protein scaffold which subsequently mineralises [20]. As Sr can influence pre-osteoblast/osteoblast behaviour [21] and mesenchymal stem cells (MSC) differentiation [22, 23], the hypothesis is that Sr would influence hDPSCs behaviour. Additionally, identifying molecular mechanisms involved in Sr mediated odontogenic differentiation of hDPSCs will substantiate the use of Sr in dentine pulp tissue engineering. Previously it has been demonstrated that Sr substituted for calcium (Ca) in bioactive glass (BG), increased osteoblast proliferation, differentiation as well as inhibiting osteoclast-mediated bone resorption [24-27]. Hence we sought to investigate the effects of Sr alone and Sr substituted BG conditioned medium (BGCM) on the odontogenic differentiation of hDPSCs, mineralising potential and related molecular mechanisms.

2. Materials and Methods:

2.1. Cell culture

Human dental pulp stem cells (hDPSCs, Lonza, Switzerland) were cultured in the Dulbecco's Modified Eagle's medium (DMEM, Lonza, Switzerland) supplemented with 10% fetal bovine serum (FBS) and antibiotics (10U/L penicillin and 100mg/L streptomycin) in a humidified atmosphere containing 10% CO_2 at 37°C with medium change every two days.

Passages 3-5 were used for all experiments. Cells were seeded in 96-well plates (1000 cells/well) for proliferation assay and ALP activity assay, or in 12-wells plates (1×10^5 cells/well) for the scratch assay. 1×10^5 cells/dish or 1×10^3 cells/dish in 10cm dishes for Western blot and colony formation respectively. 5×10^3 cells were also seeded on to sterilised cover slips and placed in 12-wells plates for immunocytochemistry. For Alizarin Red S and Sirus red staining, 24-wells plates were used with 5×10^3 cells/well cultured for 2, 3, and 4 weeks. Cells treated with odontogenic medium (OM, containing 10% FBS, 50μg/ml L-ascorbic acid, 5mM β-glycerophosphate and 10nM dexamethasone) was used as positive control for odontogenic differentiation and mineralisation study.

Sr was added to the medium of the confluent cultures at various concentrations as the chloride compound $SrCl_2.6H_2O$. The medium was then subjected to inductively coupled plasma-optical emission spectrometry (ICP-OES), to confirm the available concentrations of Sr in the medium (Fig. S1).

2.2. Cell proliferation assay

Total DNA content was measured to quantify the cellular proliferation as previously described [28]. Briefly, the plates were collected on 1, 4, 7, and 10 days after Sr (0, 0.5, 2.5, 5, 10mM) treatment, the cells washed twice with PBS and stored at -20^{o}C. With all time points collected, cells were thawed at room temperature and 100µl distilled water was added to each well, incubated for 1 hr and then refrozen. After 24 hrs they were thawed again and 100µl of the fluorochrome Hoechst 33258 at the concentration 20µg/ml in high salt TNE buffer (2M NaCl) was added to each well. The plates were read with excitation at λ 350nm and emission at λ 460nm. Cell number was calculated according to the cell number standard curve (Fig. S2A). The results were collected from three independent experiments.

2.3. Quantitative assay of ALP activity

To determine the early Sr induced differentiation of hDPSCs, ALP activity was assessed following exposure to Sr as in the cell proliferation assay. Plates were collected and washed in PBS and stored at -20^{o}C. Once all plates were collected, cells were thawed and 100µl ALP reaction solution (20mg 4-Nitropheyl-phosphate disodium salt hexahydrate tablet was dissolved in 8ml Tris buffer solution (pH=9.5) containing 15µl of 2M $MgCl_2$) was added to cell lysate, incubated in 37^{o}C for 1 hr. The resultant coloured reaction product, pNP, was measured at 405nm with a spectrophotometer. ALP activity was calculated according to the standard curve (Fig. S2B) and normalised t cell number. Experiments were performed three times.

2.4. Colony formation assay

After incubation for 14 days, cells were washed with PBS twice, fixed with formalin for 15 min, and stained with 0.5% crystal violet for 15 min at room temperature. The colony is defined to consist of at least 50 cells. Visible colonies were counted. Colony formation rate = (number of colonies/number of seeded cells) × 100%. Each experiment was repeated three times.

2.5. Scratch assay

Stem/progenitor cell migration is particularly important in tissue engineering. Therefore to study the effects of Sr on hDPSCs migration, scratch assays were performed. A confluent cell monolayer was scratched with a 200 µl pipette tip to obtain a ‘wound line’. Wounds were photographed at 0, 12, 24 and 36 hrs using an inverted microscope (Nikon, TE 2000-S, Tokyo, Japan). The images were uploaded to the WIMASIS image analysis application (https://mywim.wimasis.com/)and the wound repair (%) calculated using the following formula: wound repair (%)=100*(A-B)/A, where A is the width of cell wounds at 0 hr, and B is the width of cell wounds after incubated 12, 24 and 36 hrs. For each experiment a total four wounds were measured per treatment group, and each experiment was repeated three times.

2.6. Quantitative real-time polymerase chain reaction-qPCR

Cells were treated with Sr (0, 0.1, 1 and 2.5mM) or OM for 7 and 14 days, and total RNA was isolated using the RNeasy Mini Kit (Qiagen Biotechnology, Venlo, Netherlands). 200ng of total RNA was reverse-transcribed into cDNA using Roche Transcriptor cDNA Synthesis Kit (Roche, Basel, Switzerland). For the qPCR running, 2µl of cDNA was used for amplification of the target genes in triplicate. As well as odontogenic markers, markers more often associated with osteogenic differentiation were also measured in the treated cells. Relative expression levels of dentine sialophosphoprotein (DSPP), dentine matrix protein 1 (DMP-1), runt-related transcription factor 2 (RUNX2), osteonectin (ON), bone sialoprotein (BSP), matrix extracellular phosphoglycoprotein (MEPE), osteocalcin (OCN), bone morphogenetic protein 2 (BMP-2), and calcium sensing receptor (CaSR) were determined with glyceraldehyde 3-phosphate dehydrogenase (GAPDH) as the reference gene. The thermal cycling conditions were as follows: 95°C for 5 min and 55 cycles of 95°C for 10s, 60°C for 6s, 72°C for 6s, 76°C for 1s. LightCycler 480 SW1.5 software was used to analyse the results, utilising the fit point method. The forward and reverse primers used for PCR were designed by Roche universal probe library according to the complementary DNA sequences available in GenBank (Table 1).

Table 1: Primers for qPCR

Gene	GeneBank No.	Sequences(5'-3')	Product size
DSPP	NM_014208.3	F: ATATTGAGGGCTGGAATGGGGA	136bp
		R:TTTGTGGCTCCAGCATTGTCA	
DMP-1	NM_004407.3	F:TTTTAGGAAGTCTCGCATCT	100bp
		R: TGGGACCATCTACGTTTT	
RUNX2	NM_004348.3	F:ACTCTACCACCCCGCTGTC	96bp
		R:CAGAGGTGGCAGTGTCATCA	
ON	NM_003118.2	F:TTCCCTGTACACTGGCAGTTC	109bp
		R:AATGCTCCATGGGGATGA	
BSP	NM_004967.3	F:CAATCTGTGCCACTCACTGC	80bp
		R:CAGTCTTCATTTTGGTGATTGC	
MEPE	NM_020203.3	F:CTAAGCAAAGCTGTGTGGAAGA	77bp
		R:CTTGCCCAAATGGTGAAAA	
CaSR	NM_001178065.1	F:CGAGGAGAAAATCCTGTGGA	83bp
		R:AGTTGGAGAAGGGCACCTG	
OCN	M_34013.1	F:CTCACACTCCTCGCCCTATT	107bp
		R: TTGGACACAAAGGCTGCAC	
BMP-2	AF_040249.1	F:CACTGTGCGCAGCTTCC	107bp
		R:CCTCCGTGGGGATAGAACTT	
GAPDH	NM_002046.3	F:AGCCACATCGCTCAGACAC	66bp
		R:GCCCAATACGACCAAATCC	

2.7. Western blot analysis

For each time point (7 and 14 days), after removal of the supernatant wished with PBS the cell pellets were re-suspended in RIPA lysis buffer (containing 1% Triton X-100 and 1% cocktail proteinase inhibitors) and incubated for 15 min on ice. The protein concentration for each sample was measured using the DC™ Protein Assay (Bio-Rad, California, USA). Cell culture supernatants were collected and analysed by Western blot to determine levels of secreted DSPP and DMP-1. Coomassie blue staining was used as a loading control. Protein samples were separated by 10% sodium dodecyl sulphate polyacrylamide gel electrophoresis (130 V, 1.5 hours) and transferred onto polyvinylidene difluoride (PVDF) membranes (35 V, 1.5 hours). The membranes were blocked with 5% non-fat dry milk mixed in TBST for 1 hr, at room temperature, and then further incubated with primary antibodies overnight (Table 2). Membranes were next washed and incubated with the appropriate secondary antibody. Immunoreactive bands were visualized using the ECL kit (Roche, Basel, Switzerland). Densitometry of the observed bands and quantification was performed using ImageJ software.

Table 2: Details of Primary antibodies used in Western Blot

Antibody	Origin	Working concentration	Company
Anti-DSPP	Mouse	1:500 dilution	Santa Cruz
Anti-DMP-1	Rabbit	1:200 dilution	Abcam
Anti-p44/42 MAPK	Rabbit	1:1000 dilution	Cell Signaling Technology
Anti-Phospho-p44/42 MAPK	Mouse	1:1000 dilution	Cell Signaling Technology
Anti-β-Catenin	Mouse	1:4000 dilution	Sigma-Aldrich
GAPDH	Rabbit	1:5000 dilution	Abcam

2.8. Immunocytochemistry

Cells were fixed with ice-cold 4% paraformaldehyde for 10 min and permeablised with 0.1% Triton X-100 for 10 min. Nonspecific binding was blocked in 10% goat serum for 30 min. Primary antibodies: DSPP (1:50 dilution), DMP-1 (1:100 dilution), and rabbit anti-human dentin sialoprotein (DSP, 1:50 dilution. Santa Cruz, California, USA), rabbit anti-human cis-Golgi marker (GM130, 1:200 dilution, Abcam, Cambridge, UK), rabbit anti-human cytochrome c oxidase subunit 4 (COX4, 1:200 dilution, Abcam, Cambridge, UK), mouse anti-human mitochondrial cytochrome c oxidase subunit 2 (MTCO2, 1:200 dilution, Abcam, Cambridge, UK) and rabbit anti-human calnexin (1:200 dilution, Abcam, Cambridge, UK) were then added for 1 hr at

room temperature. Subsequently, the cells were incubated with specific secondary antibody (Alexa Fluor 568 or Alexa Fluor 488) for 1 hr at 37°C and then counter stained for nuclei using DAPI. Finally, the cells were washed and mounted on slides and viewed under Confocal (LSM710, Zeiss). The images were then analysed with ImageJ software or Zeiss microscope software ZEN.

2.9. Sirius Red staining

Sirius Red staining is presented as a method for demonstrating collagen formation. Cells were fixed with 4% glutaraldehyde at 2, 3 and 4 week time points and subsequently stained with 0.1% Sirius red dissolved in 1.3% picric acid for 1 hr at room temperature. Stained samples were washed with distilled water three times to remove unbound stain and kept at 4^{o}C. To quantify the amount of stain, and thus collagen present, collagen-bound stain was removed by incubating with 0.1M NaOH solution for 1 hr and the absorbance of the supernatant determined at 560 nm. The data were collected from three wells for each time point.

2.10. Alizarin Red S staining

After 2, 3, and 4 weeks, cells were washed with PBS and fixed in 4% glutaraldehyde for 30 min, then stained with 2% Alizarin Red S (Sigma-Aldrich, St Louis, MO, USA) for 1 hr at room temperature. Following three washings with distilled water to remove unbound stain, the cells were air-dried before being photographed. For quantification, stain was extracted with 10% cetylpyridinum chloride in deionized water incubated for 1 hr at room temperature, and the absorbance of the supernatant was measured at 560 nm. The data were collected from three same conditioned wells.

2.11. Preliminary study of novel Sr substituted BG

2.11.1. Bioactive glass design and synthesis

BGs containing SiO_2-P_2O_5-CaO-Na_2O-ZnO where calcium (Ca) was substituted with Sr were produced by a melt-quench route as previously described [26]. Briefly, the mixtures of analytical grade SiO_2, P_2O_5, $CaCO_3$, $SrCO_3$ Na_2CO_3 and ZnO (Sigma-Aldrich, Gillingham, UK) were melted in a platinum-rhodium crucible for 1 hr at 1420°C in an electric furnace (EHF 17/3, Lenton, Hope Valley, UK), then were rapidly quenched into deionised water to prevent crystallisation. After overnight drying, the glass frits were ground and sieved to yield powders<38 μm in diameter. The amorphous structure of the glasses was assessed by powder X-ray diffraction (XRD). The compositions of BGs are shown in Table 3.

Table 3. Glass compositions in mol%, NC fixed at 2.11.

Glass	SiO2(mol%)	Na2O(mol%)	CaO(mol%)	SrO(mol%)	P2O5(mol%)	ZnO(mol%)
Sr0	35.68945	26.70108	29.40607	0	6.2034	2
Sr25	35.68945	26.70108	22.05455	7.351518	6.2034	2
Sr50	35.68945	26.70108	14.70304	14.70304	6.2034	2

Sr75	35.68945	26.70108	7.351518	22.05455	6.2034	2

2.11.2. Biological effects of Sr-bioglass on hDPSCs

1.5g/L of BG powder was added to DMEM, incubated on a roller at 37^{o}C for 24 hrs and then passed through a 0.2µm filter. The medium was supplemented as described in *section 2.1* and equilibrated in a 37 ^{o}C/10% C_2O incubator overnight before being placed on cells. The cell metabolic activity was performed as described previously [29]. The effect of BGCM on cell proliferation and ALP activity was also determined with the same methods as described in *2.2* and *2.3*.

2. 12. Statistical analysis

All data are expressed as mean ± standard deviation (SD) unless otherwise noted. Differences were considered significant at $p<0.05$, determined using one-way ANOVA with Bonferroni's post hoc multiple comparison test. Statistical analysis was performed using GraphPad Prism 5.

3. Results:

3.1. Sr induces proliferation and differentiation of hDPSCs

The effect of Sr on hDPSC proliferation was measured by a DNA fluorometric assay. As demonstrated in Fig. 1A, 2.5mM Sr treatment significantly increased cell number at 24 hrs, while 10mM Sr treatment inhibited proliferation of hDPSCs. 2.5 and 5mM Sr enhanced cell proliferation by day 4 and only 5mM Sr showed an increase in cell number by day 7. Meanwhile, the cell number in all groups further increased on day 10. The general trend is accelerated growth capability of hDPSCs when exposed to Sr (0.5, 2.5, and 5mM) by the 10-day period (Fig. 1A). However, in Sr 10mM culture, cell growth is observed until day 4 and thereafter there is no significant growth. These results suggest that Sr at low concentration can induce cell proliferation, whilst high doses will inhibit proliferation. This finding was also confirmed by doing MTT assay (Fig. S3).

By performing ALP activity assay we measured the differentiation potential of hDPSCs with Sr treatment. As shown in Fig. 1B, 2.5 and 5mM Sr enhanced ALP activity (normalised to cell number) on day 1. On day 4 and 7, the ALP activity in 0.5, 2.5 and 5mM Sr treated groups exhibit a significant (*$p<0.05$) increases when compared with the Sr 0mM group. However by day 10, the 0.5 and 2.5mM Sr treatment groups showed obvious increases in ALP activity, whereas 5 and 10mM Sr treatment reduced ALP activity in DPSCs. It is obvious that ALP activity increased over time with Sr 0, 0.5 and 2.5mM during the 10 day period. In contrast, this ALP activity trend first increased then decreased in the Sr 5 and 10mM treated group. For

this reason the concentration of Sr at 0.1, 1 and 2.5Mm were used for the subsequent differentiation and mineralisation experiments.

To corroborate similarities between osteoblastic and odontogeneic differentiation the gene expression of known osteogenic markers and ECM molecules (Runx-2, ON, OCN, BSP, MEPE, and BMP-2) were determined to indicate the differentiation of hDPSCs upon Sr treatment. After 7 days of culture, higher expression of RUNX2, OCN, MEPE and BMP-2 genes was detected in Sr 2.5mM group compared to Sr 0mM treatment (Fig. 2A, D, E, and F). Moreover, at 14 days the mRNA levels of RUNX2, OCN, MEPE, BMP-2, and ON (Fig. 2B) were up-regulated in Sr 1 and 2.5 mM group, as well as in the positive control OM treatment group. The mRNA level of BSP was not significantly affected by either Sr or OM at day 14, and the expression levels actually decreased by Sr treatment at day 7(Fig. 2C).

In addition we also determined that Sr has no effect on hDPSC colony formation and migration, whereas odontogenic medium (OM) significantly inhibited the colony formation and slowed cell migration compared with the Sr 0mM group (Fig. S4).

In combination, these results indicate that Sr treatment at 1 and 2.5mM results in the odontogenic differentiation of hDPSCs via genes indicated in the differentiation of osteoblasts.

3.2. Effects of Sr on collagen formation and mineralisation of hDPSCs

Since collagen is the most abundant protein in the dentine matrix, the demonstration of collagen can be used to indicate possible dentiongenesis *in vitro*. Therefore, Sirius red staining was performed to detect collagen generated by the hDPSCs exposed to Sr (0.1, 1 and 2.5mM). There was an increase in collagen level from 2 to 4 weeks in the Sr free group (Fig. 3A). 1 and 2.5 mM Sr promotes collagen synthesis after 2, and 3 weeks when compared to the Sr 0mM group (Fig 3B). However collagen generation was not significantly increased in hDPSCs treated with 0.1mM Sr over the 4-week period (Fig. 3B).

The mineralisation potential of hDPSCs in response to Sr treatment was assessed by Alizarin Red S staining as it binds Ca^{2+} deposits formed in extracellular matrix nodules (Fig. 3C). Consistent with collagen formation assay, Sr at 1mM and 2.5mM concentration induced a significant (*$p<0.05$) increase in the staining compared with exposure to Sr free medium by week 2, 3 and 4 in hDPSCs (Fig. 3D). It should be noted that the difference in the staining was greater by 4 weeks culture when compared to 2 and 3 weeks. At very low concentrations Sr (0.1mM) also induced mineralisation by week 4.

These results collectively indicate that Sr at the specific concentrations of 1 and 2.5mM promote both collagen formation and mineralisation of hDPSCs *in vitro*.

3.3. Sr regulates the expression and secretion of DSPP and DMP1

Immune blotting analysis revealed DSPP protein as three separate bands, having apparent molecular weights between 150 and 100kDa (Fig.4A). For DMP-1, four separate bands were observed, the smallest one at the expected protein size 37kDa, while the largest one being at above 225kDa (Fig. 4A). The other two bands were observed to be in between 225kDa-102kDa. Densitometry analysis of these bands was performed to determine the total intracellular expression and processing of both DSPP and DMP-1 proteins. The bar chart (Fig. 4C) clearly shows that DSPP expression was significantly enhanced upon all the Sr doses and OM exposure after 7 days when compared to Sr free treatment. By day 14, the expression inhibited in Sr 0.1 and 2.5mM groups, however the Sr 1mM and OM groups still promote the expression (Fig. 4C). Unlike DSPP, OM treatment increased the DMP-1 on both 7 and 14 days of culture, while all the Sr groups have no significant effects at day 7, and inhibited intracellular DMP-1 expression by day 14.

Immune blotting of hDPSCs culture supernatant revealed that both DSPP and DMP-1 were secreted by the cells into culture medium (Fig. 4B). Two separate bands were observed, one at the molecular weight of 150kDa, and another between 50 and 75kDa. However for DMP-1, only one single band was observed at molecular weight between 50 and 75kDa. Densitometry analysis of these bands revealed that at day 7 both DSPP and DMP-1 secretion was induced upon exposure to Sr at 0.1 and 1mM concentration (Fig. 4C and 4D). Sr at 1mM concentration increased secretion of both DSPP and DMP-1 by day 14.

Quantifying the mRNA level of DSPP and DMP-1 by qPCR revealed that some doses of Sr and OM treatment significantly increased DSPP and DMP1 gene expression when compared with control (Sr 0 mM) in hDPSCs (Fig.4E and 4F).

The intracellular localisation of these two proteins was characterised following treatment conditions using the immunocytochemistry technique. Confocal microscopy analysis demonstrated that DSPP localises to the Golgi in hDPSCs, whereas DMP-1 localises to both the cytosol and the nucleus (Fig. 5A and 5B). Golgi localisation of DSPP is validated by using anti-GM130, and DSPP localisation stained negative for anti-COX 4 that stains mitochondria and nucleus, as well as anti-Calnexin that stains endoplasmic reticulum (Fig. S5). Moreover the proteolytic cleaved fragment DSP also did not show any colocalisation with anti-MTCO2, a marker for mitochondria (Fig. S5A). This data implicates that Golgi localisation is necessary for DSPP processing as described previously in studies related to mutations affecting human DSPP localisation to Golgi [17]. Further 0.1mM Sr and OM treatment induces DSPP localisation to Golgi, while no apparent changes in DMP-1 localisation was observed upon Sr and OM treatment.

Taken together these immune studies imply that Sr treatment regulates DSPP and DMP-1 gene expression and secretion to induce odontogenic differentiation and mineralisation of hDSPCs.

3.4. Sr activated CaSR and downstream MAPK pathway

To explore the potential mechanism of Sr induced odontogenic differentiation, we investigated the CaSR expression in hDPSCs following Sr treatment. After 7 days in culture, 1mM Sr enhanced CaSR mRNA expression more than threefold compared with the control group (Fig. 6A). However, the expression was increased in both Sr 1 and 2.5mM groups after 14 days of culture (Fig. 6A). But no such enhancement was observed in OM group or Sr 0.1Mm group.

The Sr treated cell lysates were subjected to the detection of MAPK/ERK and Wnt/β-catenin signalling molecules, namely phosphorylated ERK (p-ERK), ERK and β-catenin by Western blot (Fig. 6B). Increased ERK phosphorylation was detected in Sr 1mM group when compared with the Sr 0 mM group after 14 days of culture (Fig. 6C). But neither Sr treatment groups nor OM had significant effects on ERK and β-catenin expression in hDPSCs (Fig. 6 D and E).

Therefore, these data suggest that CaSR and the downstream MAPK/ERK signalling pathway might play a role in Sr mediated odontogenic differentiation of hDPSCs.

3.5. Biological effects of Sr substituted BG on hDPSCs

The XRD patterns (Fig. 7A) confirm that all the glasses were amorphous, with an amorphous halo centred on 32° 2θ. It is also evident that the traces of the glasses with higher Sr content have higher intensities and are shifted more to lower 2θ values.

Total MTT activity per well data (Fig. 7B) indicates that these novel BGs increased cell metabolic activity at late time points (7 and 10 days) but not at early time points (1 and 4 days). On day 7, compared with negative control group MTT activity was increased in Sr 50 and 75 groups. By day 10, the MTT activity in all groups had increased, meanwhile Sr 0, 50 and 75 groups showed a pronounced increase. Conversely, cell growth of hDPSCs was inhibited by BGCM after 4, 7 and 10 days of culture when compared with the control group. However, ALP activity of hDPSCs was enhanced by BGCM after 7 and 10 days treatment, but no effect on ALP activity was evident at early time points (1 and 4 days) as shown in Fig. 7D.

4. Discussion:

Biomaterials with potential clinical applications in regenerative dentinogenesis should provide optimal conditions for cell adhesion, migration, proliferation and differentiation of dental pulp cells into functional odontoblasts. Recently, Sr has attracted attention owing to its beneficial effects on bone repair [30-32]. Sr can induce the differentiation of MSCs into osteoblasts [21], but could Sr also induce the differentiation of dental pulp stem cells into odontoblasts? This would open a new avenue for regulating dentine mass and maintaining tooth viability. The present

investigation demonstrates for the first time, the potential use of Sr for stimulating hDPSCs in dentine regeneration. Here we show that Sr induces proliferation and differentiation of hDPSCs (Fig. 1). The observed ALP activity with Sr treatment over time indicates the differentiation potential of hDPSCs. To further examine the influences of Sr on odontogenesis of hDPSCs, mRNA expression levels of RUNX2, ON, BSP, MEPE, OCN and BMP-2 were chosen as markers for the odontogenic phenotype. Among these, RUNX2 is a transcriptional factor and known master regulator in controlling odontoblasts differentiation via regulating the expression of genes that are required for odontoblastic differentiation [48]. The others are non-collagenous proteins in dentine matrix and play fundamental roles in actively promoting, controlling, and regulating odontogenic differentiation, mineralisation, and crystal growth during dentinogenesis [49]. These genes are also considered as osteogenic markers. qPCR data showed that hDPSCs cultured with Sr had increased mRNA levels of RUNX2, OCN, MEPE and BMP-2 at 7 days and 14 days, and ON at 14 days only, when compared to those cultured without Sr (Fig. 2). BSP levels were not affected by Sr treatment. These findings suggested that Sr enhanced the differentiation of the hDPSCs in a fashion with similarities to osteoblast differentiation, and might also impact on mineralisation potential for tertiary dentine formation. Therefore, collagen formation and mineralisation were studied subsequently. Collagen is the most abundant protein in dentine, and it plays a fundamental role in biomineralisation [33]. Thus formation of collagen is critical to assess odontogenic differentiation of hDPSCs. Increase in collagen formation and mineralisation was shown to be promoted by administration of Sr in hDPSCs culture (Fig. 3). These findings lend support to the idea that even low doses Sr can promote the collagen and mineralised nodule formation through increase in proliferation and differentiation potential of hDPSCs.

Molecular characterisation of Sr-elicited effects revealed its role in regulation of DSPP and DMP-1 expression and secretion (Fig. 4). DSPP and DMP-1 are highly phosphorylated proteins that belong to the family of small integrin-binding ligand N-linked glycoproteins (SIBLINGs) [34]. During dentinogenesis, DSPP is proteolytically cleaved into small subunits-dentine sialoprotein (DSP), dentine phosphoprotein (DPP) [35, 36], and also dentine glycoprotein (DGP) which is a third, and recently identified, fragment [37]. Consistent with a previous study [38], three separate bands were observed for DSPP in our study. The molecular weight of these three bands indicates that the highest one (150kDa) as full-length DSPP with the other two being the cleavage products-DSP and DPP (Fig. 4A). Densitometry analysis revealed that at day 7, both Sr and OM induced DSPP expression and processing (Fig. 4C). It has been suggested that the proteolytic processing of DSPP into DPP and DSP is the activating stage in the mechanism of DSPP function [39, 40]. Various studies have shown that DPP is important in the formation and growth of apatite during biomineralisation [41, 42]. On the other hand, DSP has been shown to be involved in the initiation of mineralisation, but has no functional role in the maturation of the mineralised crystals [36, 43]. In our case, both intracellular and extracellular DSPP

was increased upon Sr administration (0.1 and 1mM) treatment (Fig. 4). Furthermore, DSPP localisation to Golgi was identified by immunocytochemistry. 0.1mM Sr induces the localisation to the Golgi. This implies Sr promotes hDPSCs mineralisation via increasing DSPP protein expression and processing via Golgi prior to secretion (Fig. 5C).

Unlike DSPP, four separated bands were observed in DMP-1 blotting. Previous studies have demonstrated that DMP-1 is processed into two fragments: N-terminal fragment with the molecular weight 37 kDa and C-terminal fragment which is 57 kDa [44-46]. This is consistent with our results (Fig. 4), which showed one band at 37kDa intracellularly and one band between 50 and 75kDa extracellularly. However, it is reported that the molecular weight of full length DMP-1 is around 106-kDa [47], while in our study one band with the molecular weight above 225kDa was detected, this suggests the formation of possibly a DMP-1 protein dimer, though it has also been associated with protein glycosylation [48]. Only an increase in DMP-1 secretion of with Sr treatment was determined, with no change in the intercellular DMP-1 signal. However, when we performed qPCR, we found that at day 7 both Sr and OM treatment promoted DMP-1 expression at the mRNA level. These results implicate that DMP-1 levels are tightly controlled intracellularly by maintaining its turnover and the secretory potential is induced upon cleavage. As reported the native full length form of DMP-1 inhibits mineralisation, whilst when cleaved and dephosphorylated, it initiates mineralisation [49]. Based on these results it is quite tempting to speculate that low Sr concentrations can regulate the tight expression of intracellular DMP-1, with no impact on its intracellular localisation (Fig. 5) and also promotes its secretion to induce mineralisation.

The activation of the CaSR by Sr in osteoblasts that leads to activation of the downstream signalling pathways including mitogen-activated protein kinases (MAPKs), and Wnt/β-catenin is well established [18, 19]. However, no such studies have investigated the mechanisms related to Sr effects on hDPSCs or odontoblasts. Here we first report that CaSR is also expressed in hDPSCs and expression levels increase with Sr treatment, especially Sr at 1mM dose. Moreover, by determining the protein levels of p-ERK, ERK and β-catenin we found the p-ERK was up regulated by Sr 1mM treatment, while there was no distinguishable difference in ERK and β-catenin levels between Sr treated group and control group (Fig. 6). This indicated that Sr is an agonist of the CaSR and that this receptor could be involved in mediating the biological effects of Sr in hDPSCs. In addition, MAPK/ERK might act as the downstream signalling pathway of CaSR in Sr induced odontogenic differentiation rather than Wnt/beta catenin pathway. However, further studies are required to fully understand the mechanisms involved in the Sr effects on hDPSCs.

Ca has been reported to act as a network modifier in silicate bioactive glass system. As Sr has a similar charge and ionic radius to Ca, when it is substituted into the glass network, it may play a similar role. In this study we successfully created a group of Sr containing BGs without changing the network connectivity. At early time

points (1 and 4 days), the metabolic activity of hDPSCs treated with BGCM was not significantly different from that observed in cells treated with standard culture medium. This suggests that the dissolution products of these novel glasses are at least non-cytotoxic. However, after 7 and 10 days in culture, BGCM from some glasses enhanced the metabolic activity compared with the control group. We also noted that the MTT activity in cells treated with BGCM from high Sr containing glasses (Sr 50 and 75%) was higher than CM from the Sr free glass. This finding suggests that the high Sr containing BGCM enhance metabolic activity in hDPSCs than that caused by the presence of BGCM from Sr free glass. This might be explained by the presence of Sr ions in the medium. Similarly, our data also showed that BGCM from Sr substituted BG dose-dependently enhanced the ALP activity when compared with the control group. This result is in agreement with the data showed in 3.1. However, the cell growth was inhibited upon BGCM treatment, the mechanism by which in the present study is not clear.

5. Conclusion:

DSPP and DMP-1 are the main molecular drivers of odontogenic differentiation in hDPSCs. Our results suggest that Sr modulates the expression and secretion of these proteins in vitro via the CaSR using a pathway with similarities to osteoblast differentiation. Sr also increased matrix production and mineralisation. Additionally, Sr substituted bioglass increased hDPSCs metabolic and ALP activities. Sr added to dental applications could have the potential to differentiate dental pulp stem cells to induce dentine-like matrix formation. Therefore, given these effects on hDPSCs, the consequence of added Sr to dental materials needs to be reconsidered, and whether Sr has therapeutic potential warrants further investigation.

Acknowledgements

The Authors would like to thank Dr. Teh, Muy-Teck and Dr Hong Wan for the helpful discussions during the course of this study.

Mei Huang is supported by China Scholarship Council (CSC)/Queen Mary University of London Joint PhD scholarships.

References

[1] Li Y, Shu L-H, Yan M, Dai W-Y, Li J-J, Zhang G-D, et al. Adult stem cell-based apexogenesis. World Journal of Methodology 2014;4:99-108.
[2] Listl S, Galloway J, Mossey PA, Marcenes W. Global Economic Impact of Dental Diseases. J Dent Res 2015;94:1355-61.

[3] Nakashima M RA. The application of bone morphogenetic proteins to dental tissue engineering. Nature Biotechnology 2003;21:1025-32.
[4] Ikada Y. Challenges in tissue engineering. Journal of the Royal Society Interface 2006;3:589-601.
[5] Gronthos S MM, Brahim J, Robey PG, Shi S. Postnatal human dental pulp stem cells (DPSCs) in vitro and in vivo. Proceedings of the National Academy of Sciences 2000;97:13625-30.
[6] Gronthos S BJ, Li W, Fisher LW, Cherman N, Boyde A, DenBesten P, Robey PG, Shi S. Stem Cell Properties of Human Dental Pulp Stem Cells. Journal of Dental Research 2002;81:531-5.
[7] Wang J, Ma H, Jin X, Hu J, Liu X, Ni L, et al. The effect of scaffold architecture on odontogenic differentiation of human dental pulp stem cells. Biomaterials 2011;32:7822-30.
[8] Lee J-H, Lee D-S, Choung H-W, Shon W-J, Seo B-M, Lee E-H, et al. Odontogenic differentiation of human dental pulp stem cells induced by preameloblast-derived factors. Biomaterials 2011;32:9696-706.
[9] Zheng L, Yang F, Shen H, Hu X, Mochizuki C, Sato M, et al. The effect of composition of calcium phosphate composite scaffolds on the formation of tooth tissue from human dental pulp stem cells. Biomaterials 2011;32:7053-9.
[10] Paduano F, Marrelli M, White LJ, Shakesheff KM, Tatullo M. Odontogenic Differentiation of Human Dental Pulp Stem Cells on Hydrogel Scaffolds Derived from Decellularized Bone Extracellular Matrix and Collagen Type I. PLoS ONE 2016;11:e0148225.
[11] Bohl KS, Shon J, Rutherford B, Mooney DJ. Role of synthetic extracellular matrix in development of engineered dental pulp. J Biomater Sci Polym Ed 1998;9:749-64.
[12] Rezwan K, Chen QZ, Blaker JJ, Boccaccini AR. Biodegradable and bioactive porous polymer/inorganic composite scaffolds for bone tissue engineering. Biomaterials 2006;27:3413-31.
[13] Seo MS, Hwang KG, Lee J, Kim H, Baek SH. The effect of mineral trioxide aggregate on odontogenic differentiation in dental pulp stem cells. J Endod 2013;39:242-8.
[14] Estrela C, Holland R. Calcium hydroxide: study based on scientific evidences. J Appl Oral Sci 2003;11:269-82.
[15] Holland R, Pinheiro CE, de Mello W, Nery MJ, de Souza V. Histochemical analysis of the dogs' dental pulp after pulp capping with calcium, barium, and strontium hydroxides. J Endod 1982;8:444-7.
[16] Stamboulis A LR, Hill RG. Characterisation of commercial ionomer glasses using magic angle nuclear magnetic resonance (MAS-NMR). Biomaterials 2004;25:3907-13.
[17] Verberckmoes SC DBM, D'Haese PC. Dose-dependent effects of strontium on osteoblast function and mineralization. Kidney Int 2003;64:534-43.
[18] Fromigue O, Hay E, Barbara A, Petrel C, Traiffort E, Ruat M, et al. Calcium sensing receptor-dependent and receptor-independent activation of osteoblast replication and survival by strontium ranelate. J Cell Mol Med 2009;13:2189-99.
[19] Rybchyn MS, Slater M, Conigrave AD, Mason RS. An Akt-dependent increase in canonical Wnt signaling and a decrease in sclerostin protein levels are involved in strontium ranelate-induced osteogenic effects in human osteoblasts. J Biol Chem 2011;286:23771-9.
[20] Boskey AL. Mineralization of Bones and Teeth. Elements 2007;3:385-91.
[21] Choudhary S, Halbout P, Alander C, Raisz L, Pilbeam C. Strontium ranelate promotes osteoblastic differentiation and mineralization of murine bone marrow stromal cells: involvement of prostaglandins. J Bone Miner Res 2007;22:1002-10.
[22] Yang F, Yang D, Tu J, Zheng Q, Cai L, Wang L. Strontium enhances osteogenic differentiation of mesenchymal stem cells and in vivo bone formation by activating Wnt/catenin signaling. Stem Cells 2011;29:981-91.
[23] Yang F, Tu J, Yang D, Li G, Cai L, Wang L. Osteogenic differentiation of mesenchymal stem cells could be enhanced by strontium. Conf Proc IEEE Eng Med Biol Soc 2010;2010:823-6.
[24] Gentleman E, Fredholm YC, Jell G, Lotfibakhshaiesh N, O'Donnell MD, Hill RG, et al. The effects of strontium-substituted bioactive glasses on osteoblasts and osteoclasts in vitro. Biomaterials 2010;31:3949-56.

[25] O'Donnell MD, Hill RG. Influence of strontium and the importance of glass chemistry and structure when designing bioactive glasses for bone regeneration. Acta Biomater 2010;6:2382-5.
[26] Fredholm YC, Karpukhina N, Brauer DS, Jones JR, Law RV, Hill RG. Influence of strontium for calcium substitution in bioactive glasses on degradation, ion release and apatite formation. J R Soc Interface 2012;9:880-9.
[27] Brauer DS, Karpukhina N, Kedia G, Bhat A, Law RV, Radecka I, et al. Bactericidal strontium-releasing injectable bone cements based on bioactive glasses. J R Soc Interface 2012.
[28] Rago R MJ, Wilding G. DNA fluorometric assay in 96-well tissue culture plates using hoechst 33258 after cell lysis by freezing in distilled water. Analytical Biochemistry 1900;191:31-4.
[29] Gentleman E FY, Jell G, Lotfibakhshaiesh N, O'Donnell MD, Hill RG, Stevens MM. The effects of strontium-substituted bioactive glasses on osteoblasts and osteoclasts in vitro. Biomaterials 2010;31:3949-56.
[30] Aaseth J BG, Andersen O. Osteoporosis and trace elements – An overview. Journal of Trace Elements in Medicine and Biology 2012;26:149-52.
[31] Marie PJ, Ammann P, Boivin G, Rey C. Mechanisms of Action and Therapeutic Potential of Strontium in Bone. Calcified tissue international 2001;69:121-9.
[32] Marie PJ. Strontium ranelate: New insights into its dual mode of action. Bone 2007;40:S5-S8.
[33] Goldberg M KA, Young M, Boskey A. Dentin Structure, Composition and Mineralization. Front Biosci 2011;1:711-35.
[34] Suzuki S, Haruyama N, Nishimura F, Kulkarni AB. Dentin sialophosphoprotein and dentin matrix protein-1: Two highly phosphorylated proteins in mineralized tissues. Archives of Oral Biology 2012;57:1165-75.
[35] von Marschall Z, Fisher LW. Dentin sialophosphoprotein (DSPP) is cleaved into its two natural dentin matrix products by three isoforms of bone morphogenetic protein-1 (BMP1). Matrix Biology 2010;29:295-303.
[36] Yamakoshi Y. Dentinogenesis and Dentin Sialophosphoprotein (DSPP). Journal of Oral Biosciences 2009;51:134-42.
[37] Yamakoshi Y, Hu JC, Fukae M, Zhang H, Simmer JP. Dentin glycoprotein: the protein in the middle of the dentin sialophosphoprotein chimera. J Biol Chem 2005;280:17472-9.
[38] Sun Y, Lu Y, Chen S, Prasad M, Wang X, Zhu Q, et al. Key proteolytic cleavage site and full-length form of DSPP. J Dent Res 2010;89:498-503.
[39] Zhang X, Zhao J, Li C, Gao S, Qiu C, Liu P, et al. DSPP mutation in dentinogenesis imperfecta Shields type II. Nat Genet 2001;27:151-2.
[40] Qin C, Baba O, Butler WT. Post-translational modifications of sibling proteins and their roles in osteogenesis and dentinogenesis. Crit Rev Oral Biol Med 2004;15:126-36.
[41] Boskey AL, Maresca M, Doty S, Sabsay B, Veis A. Concentration-dependent effects of dentin phosphophoryn in the regulation of in vitro hydroxyapatite formation and growth. Bone Miner 1990;11:55-65.
[42] He G, Ramachandran A, Dahl T, George S, Schultz D, Cookson D, et al. Phosphorylation of phosphophoryn is crucial for its function as a mediator of biomineralization. J Biol Chem 2005;280:33109-14.
[43] Boskey A SL, Tan M, Doty SB, Butler WT. Dentin sialoprotein (DSP) has limited effects on in vitro apatite formation and growth. Calcif Tissue Int 2000;67:472-8.
[44] Qin C, Brunn JC, Cook RG, Orkiszewski RS, Malone JP, Veis A, et al. Evidence for the proteolytic processing of dentin matrix protein 1. Identification and characterization of processed fragments and cleavage sites. J Biol Chem 2003;278:34700-8.
[45] Deshpande AS FP, Zhang X, Jayaraman T, Sfeir C, Beniash E. Primary Structure and Phosphorylation of Dentin Matrix Protein 1 (DMP1) and Dentin Phosphophoryn (DPP) Uniquely Determine Their Role in Biomineralization. Biomacromolecules 2011;12:2933-45.
[46] Sun Y CL, Ma S, Zhou J, Zhang H, Feng JQ, Qin C. Roles of DMP1 Processing in Osteogenesis, Dentinogenesis and Chondrogenesis. Cells Tissues Organs 2011;194:199-204.

[47] Gericke A, Qin C, Sun Y, Redfern R, Redfern D, Fujimoto Y, et al. Different forms of DMP1 play distinct roles in mineralization. J Dent Res 2010;89:355-9.
[48] Kim JW, Yamakoshi Y, Iwata T, Hu YY, Zhang H, Hu JC, et al. Porcine dentin matrix protein 1: gene structure, cDNA sequence, and expression in teeth. Eur J Oral Sci 2006;114:33-41.
[49] Tartaix PH, Doulaverakis M, George A, Fisher LW, Butler WT, Qin C, et al. In vitro effects of dentin matrix protein-1 on hydroxyapatite formation provide insights into in vivo functions. J Biol Chem 2004;279:18115-20.

Figure Legends:

Figure 1. Sr induces proliferation and ALP activity of hDPSCs

(A): Cell proliferation study of hDPSCs treated with/without Sr. The total DNA contents were measured on day 1, 4, 7, and 10. Values shown are mean±SD for triplicate cultures. *p<0.05 = significant difference compared with Sr 0mM group.

(B): The ALP activity per cell of hDPSCs under Sr treatments was determined by colorimetric assay on day 1, 4, 7, and 10. Values shown are mean±SD for triplicate cultures. *p<0.05 = significant difference compared with Sr 0mM group.

Figure 2. Effects of Sr on gene expression of odontogenic/osteogenic differentiation markers in hDPSCs.

(A)-(F): qPCR analysis of RUNX2, ON, BSP, OCN, MEPE and BMP-2 mRNA expression in DPSCs following culture for 7 and 14 days exposure to series Sr dose (0, 0.1, 1, 2.5mM) and OM. Levels were normalized to the reference gene - GAPDH. Data are expressed as a relative change compared with Sr 0mM group. Values shown are mean±SD for triplicate cultures *p<0.05 or **p<0.01 = significant difference compared with Sr 0mM group.

Figure 3. Effects of Sr on collagen formation and mineralisation of hDPSCs cultured for 2, 3, and 4 weeks.

(A): Photographs of sirius red stained for collagen (in orange colour) of cultures in a 24-wells plate.

(B): Quantification of sirius red staining of DPSCs cultures. Data are expressed as a relative change compared with Sr 0mM group. Values shown are mean±SD for triplicate cultures *p<0.05 = significant difference compared with Sr 0mM group.

(C): Photographs of Alizarin Red S stained mineralization (in red colour) of cultures in a 24-wells plate.

(D): Quantification of Alizarin Red S staining of DPSCs cultures. Data are expressed as a relative change compared with Sr 0mM group. Values shown are mean±SD for triplicate cultures *p<0.05 = significant difference compared with Sr 0mM group.

Figure 4. Strontium regulates DSPP and DMP-1 expression and secretion

hDPSCs were cultured with/without Sr for 7 and 14 days, and DSPP and DMP-1 expression and secretion were assessed by western blot and qPCR.

(A): Intracellular DSPP and DMP-1 was measured by western blot with specific antibodies, GAPDH was used here as loading control. Lane1: negative control, cells cultured in DMEM without Sr; lane 2: Cell cultured with OM; lane3-lane 5: Cells exposure in Sr 0.1mM, 1mM and 2.5mM conditioned medium.

(B): Secretion DSPP and DMP-1 in culture supernatant was determined by Western blot. Coomassie blue staining of the supernatant was used to control the sample loading. The lanes setup is same as in (A).

(C): Relative intensity of intracellular DSPP and DMP-1 to loading control GAPDH were obtained, and then compared to that of Sr 0mM group, fold changes are showing on the bar chart. Values shown are mean±SD for triplicate cultures *p<0.05 or **p<0.01 = significant difference compared with Sr 0mM group.

(D): Relative intensity of secreted DSPP and DMP-1 to Coomassie blue staining were obtained, and then compared to that of Sr 0mM group, fold changes are showing on the bar chart. Values shown are mean±SD for triplicate cultures *p<0.05 or **p<0.01 = significant difference compared with Sr 0mM group.

(E) and (F): qPCR analysis of DSPP (E) and DMP-1 (F) mRNA expression in DPSCs following culture for 7 and 14 days exposure to series Sr dose (0, 0.1, 1, 2.5mM) and OM. Levels were normalized to the reference gene-GAPDH. Data are expressed as a relative change compared with Sr 0mM group. Values shown are mean±SD for triplicate cultures *p<0.05 or **p<0.01 = significant difference compared with Sr 0mM group.

Figure 5. Subcellular localisation of DSPP and DMP-1 in hDPSCs.

(A): Representative images of DSPP and DMP-1 staining of hDPSCs upon Sr treatment for 7 days. DSPP (red) and DMP-1 (green) and cell nuclei (blue). White arrow points to the distinct nuclear localization of DSPP, while yellow arrow points to the peri nuclear localisation of DSPP. Scale bar = 50µm. Images presented are representative n=100 cells in different fields of view from three different experiments.

(B): The co-localisation of DSPP (Green) and Golgi stained by GM130 (red) in hDPSCs. Images were captured under LSM710 Meta Confocal microscopy. Scale bar for 40x indicates 50µm and for 100x image indicates 8µm. Images presented are representative n=100 cells in different fields of view from three different experiments.

(C): Bar chart represents the percentage of cells with the DSPP colocalisation with GM130 in Golgi. *p<0.05 = significant difference of colocalisation in experimental samples compared with Sr 0mM group.

Figure 6. Involvement of CaSR and MAPK/ERK signalling pathway in hDPSCs upon Sr treatment.

(A): qPCR analysis of CaSR mRNA expression in DPSCs following culture for 7 and 14 days exposure to series Sr dose (0, 0.1, 1, 2.5mM) and OM. Levels were normalized to the reference gene - GAPDH. Data are expressed as a relative change compared with Sr 0mM group. Values shown are mean±SD for triplicate cultures *p<0.05 or **p<0.01 = significant difference compared with Sr 0mM group.

(B): p-ERK, ERK, and β-catenin was measured by Western blot with specific antibodies, GAPDH was used as loading control. Lane1: negative control, cells cultured in DMEM without Sr; lane 2: Cell cultured with OM; lane3-lane 5: Cells exposure in Sr 0.1mM, 1mM and 2.5mM conditioned medium.

(C)-(E): Relative intensity of p-ERK, ERK, and β-catenin to loading control GAPDH were obtained, and then compared to that of Sr 0mM group, fold changes are showing on the bar chart. Values shown are mean±SD for triplicate cultures *p<0.05 or **p<0.01 = significant difference compared with Sr 0mM group.

Figure 7. Biological effects of Sr substituted BG on hDPSCs.

(A): XRD patterns of all unreacted BG confirming amorphous nature.

(B): Normalised MTT activity of hDPSCs treated with BGCM. Data are expressed as a relative change compared with negative control group after 1 day in culture. Values shown are mean±SD for triplicate cultures. *p<0.05 = significant difference compared with negative control group.

(C): Cell proliferation study of hDPSCs treated with/ without BGCM. The total DNA contents were measured on day 1, 4, 7 and 10. Values shown are mean±SD for triplicate cultures. *p<0.05= significant difference compared with negative control group.

(D): ALP activity of hDPSCs under Sr substituted BGCM. The ALP activity was determined by colorimetric assay on day 1, 4, 7, and 10. Values shown are mean±SD for triplicate cultures. *p<0.05 = significant difference compared with negative control group.

Figure(s)

Click here to download high resolution image

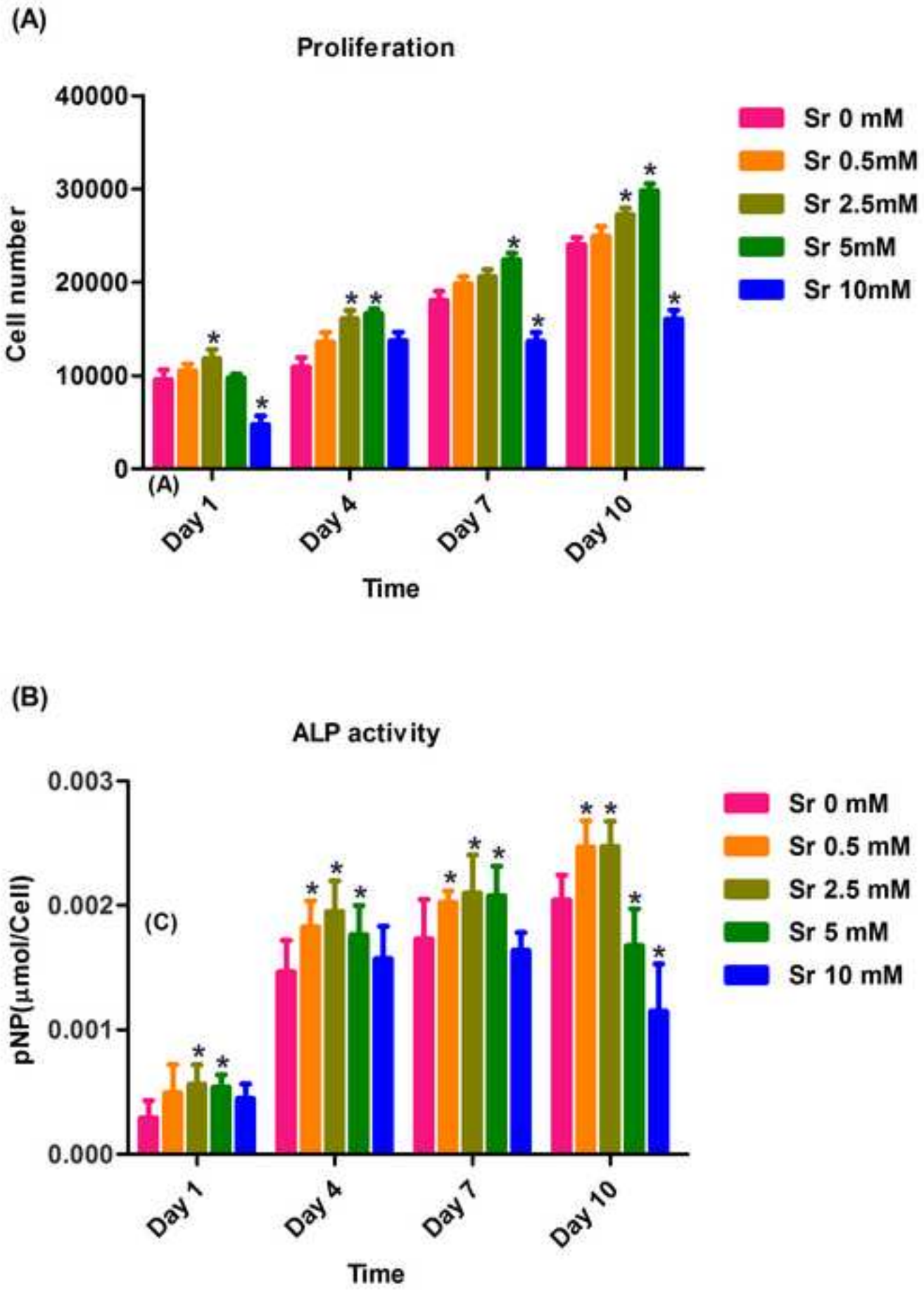

Figure(s)

Click here to download high resolution image

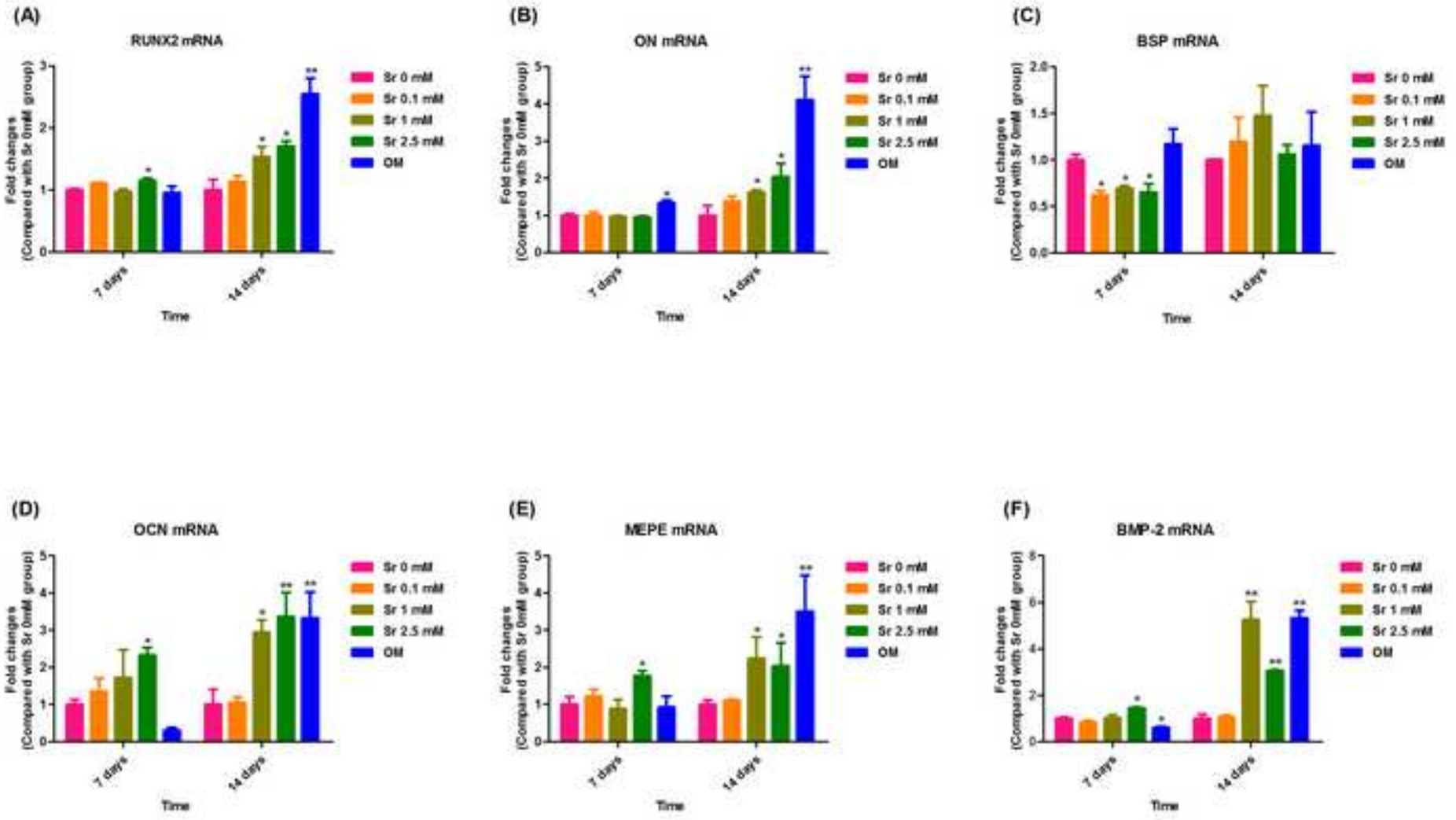

Figure(s)

Click here to download high resolution image

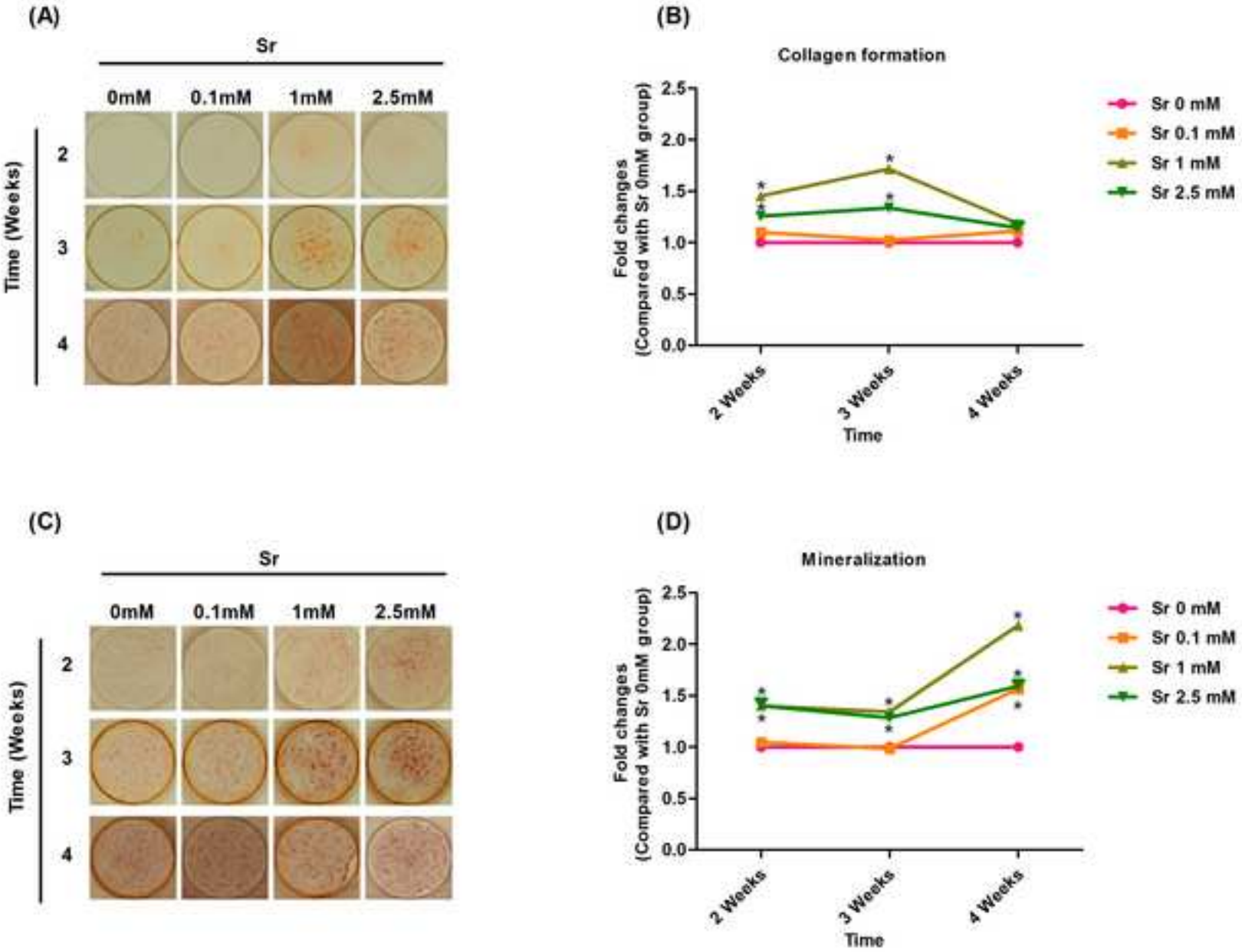

Figure(s)

Click here to download high resolution image

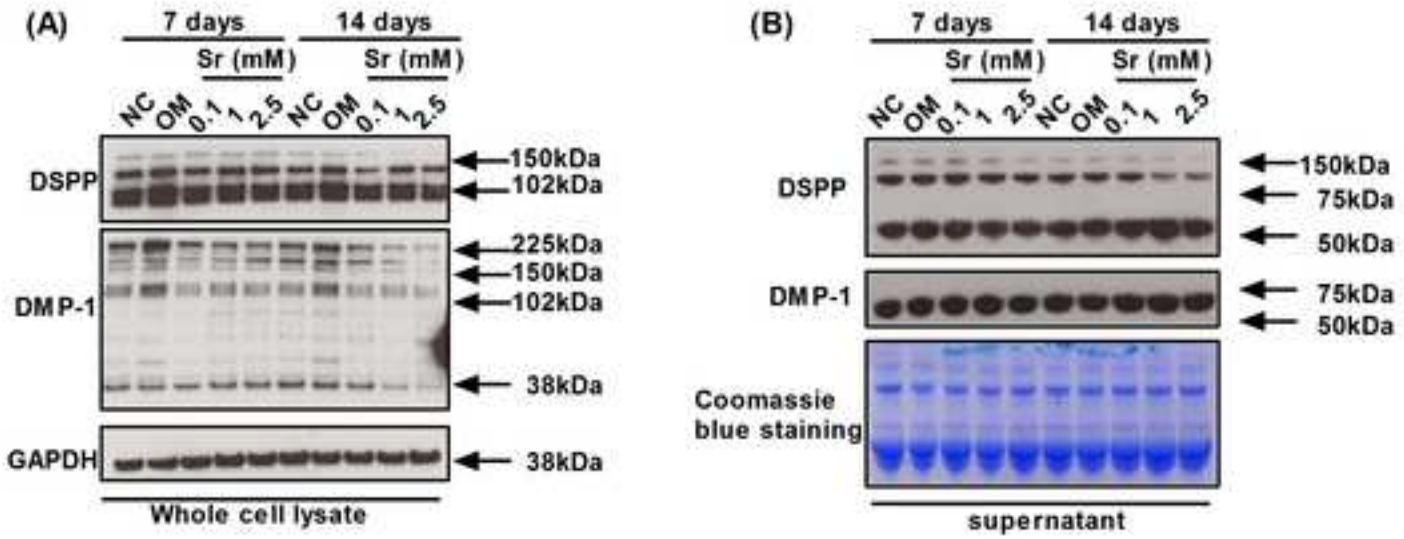

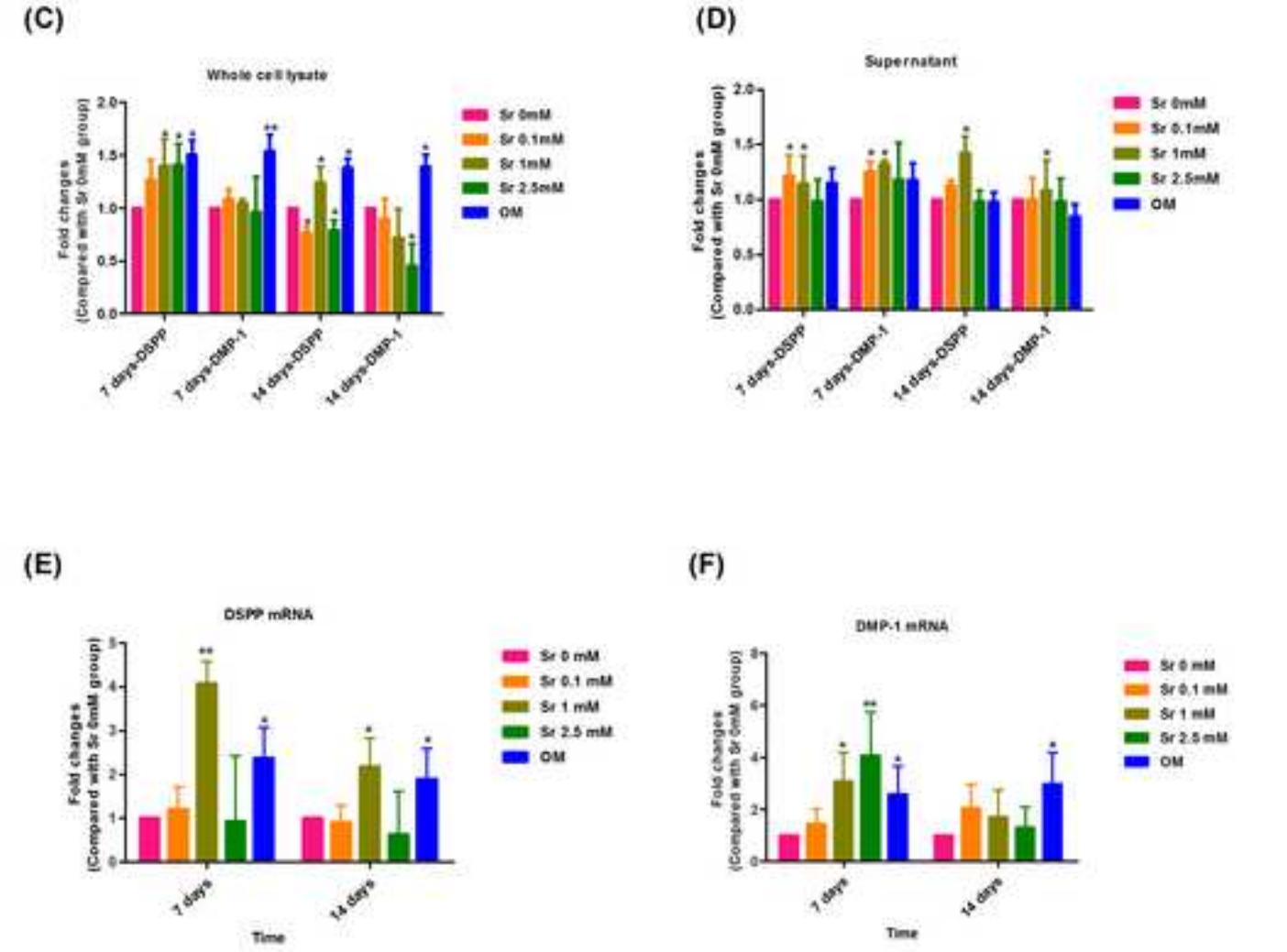

Figure(s)

Click here to download high resolution image

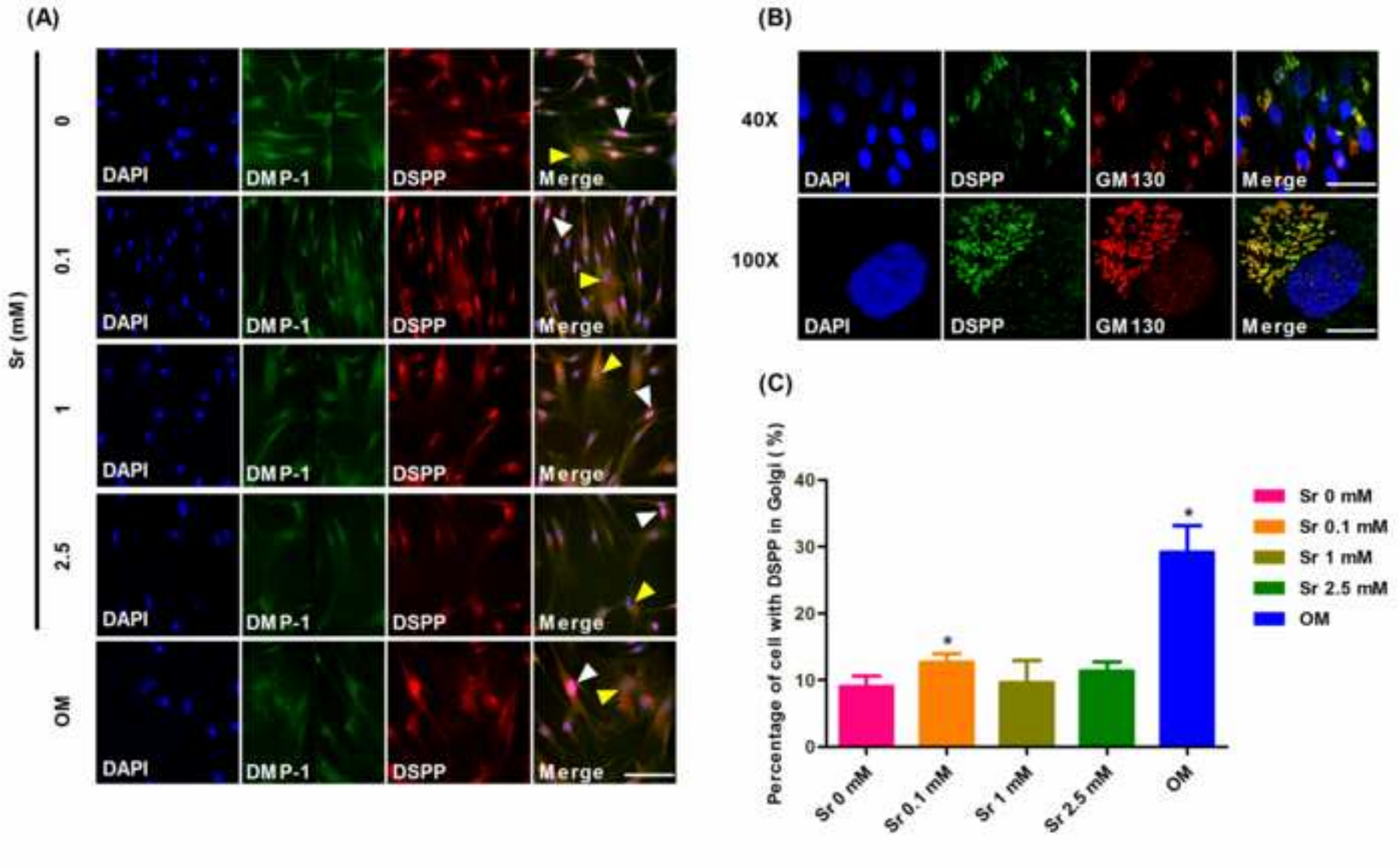

Figure(s)

Click here to download high resolution image

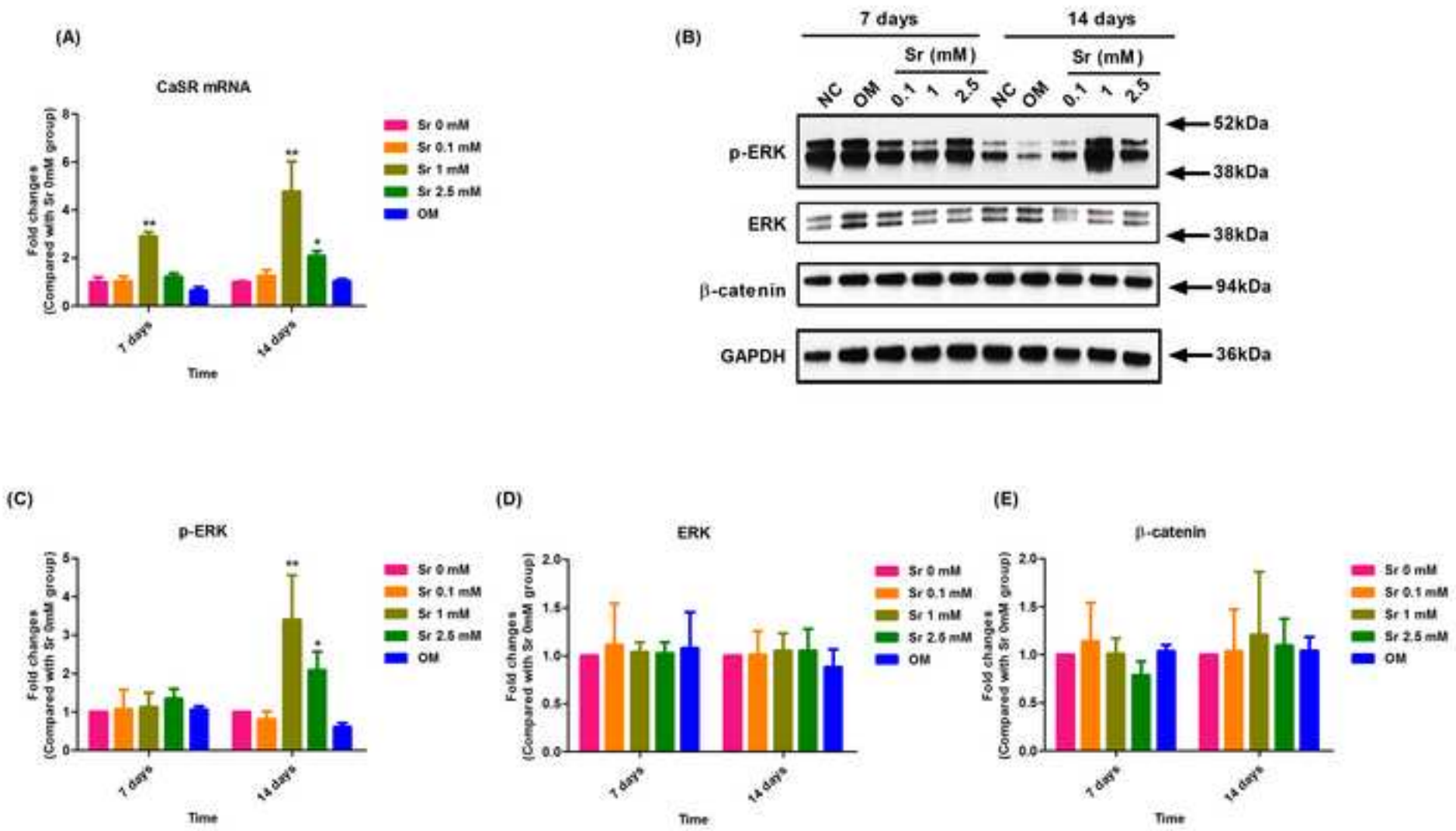

Figure(s)

Click here to download high resolution image

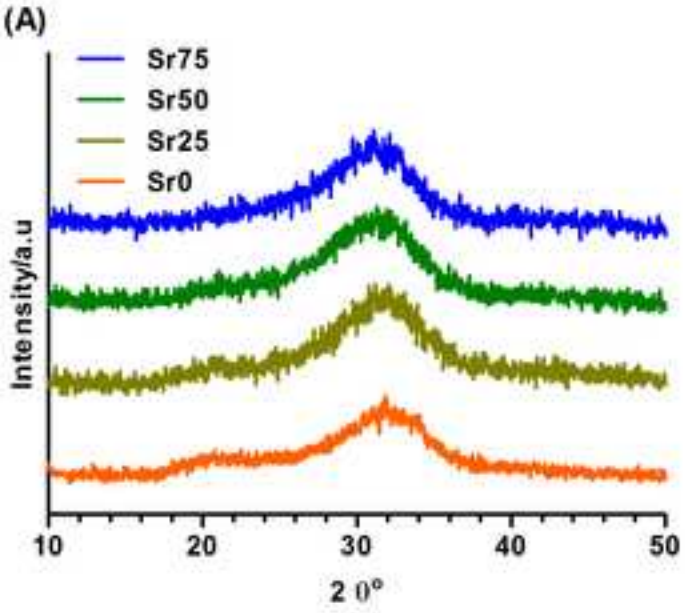

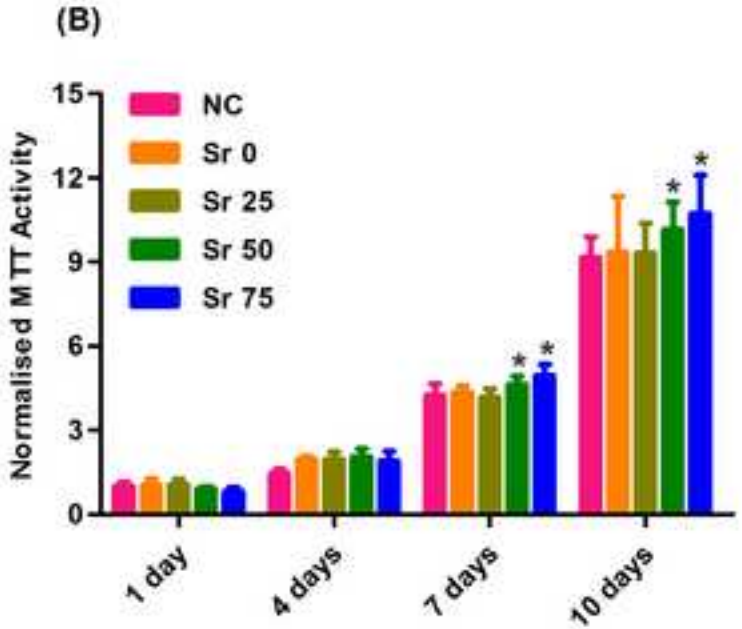

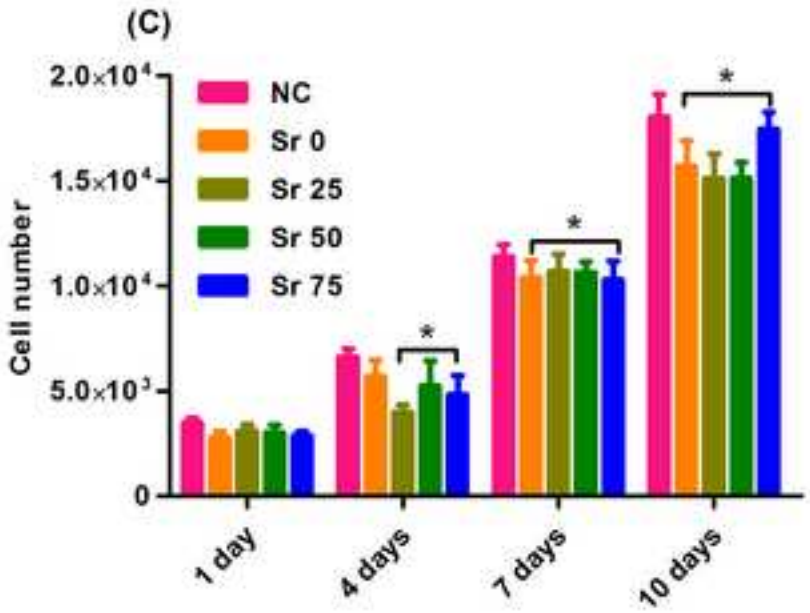

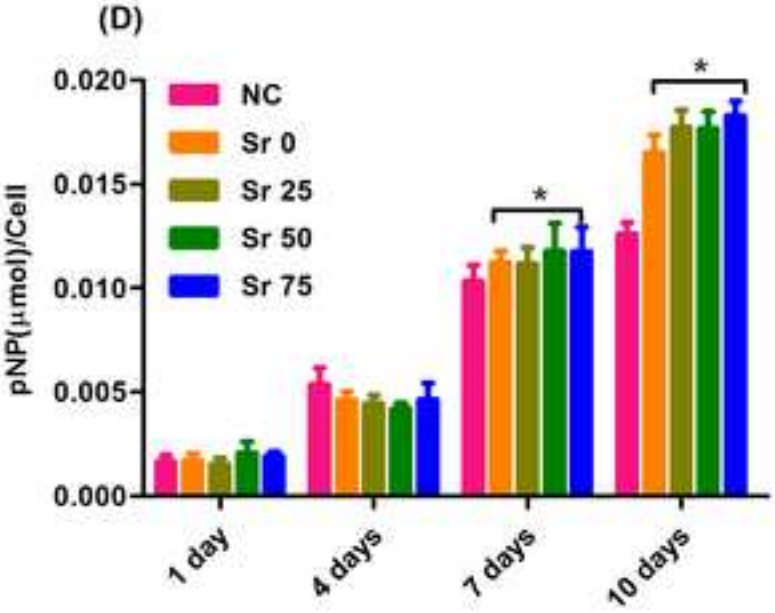

Supplementary Material

Click here to download Supplementary Material: supplementary material.docx